WATER RESOURCES RESEARCH, VOL. 26, NO. 5, PAGES 1001–1012, MAY 1990

Modeling of Meltwater Infiltration in Subfreezing Snow

TISSA H. ILLANGASEKARE AND RODNEY J. WALTER, JR.

Department of Civil, Environmental and Architectural Engineering, University of Colorado, Boulder

MARK F. MEIER AND W. TAD PFEFFER

Institute for Arctic and Alpine Research, University of Colorado, Boulder

A mathematical model which incorporates the processes that influence water flow and heat transfer in subfreezing snow was developed. Among the aspects of snow included are density and grain-size heterogeneities, capillary-pressure gradients, meltwater refreezing, time dependent hydraulic and thermal parameters, and heat conduction. From this conceptual mathematical model a numerical model of two-dimensional meltwater infiltration was developed. Results from various test cases show which data are most important to measure accurately in the field, in order to determine how the snowpack will respond to an introduction of meltwater. These simulations also show the importance of the orientation of the various layers which make up the snowpack and how randomly distributed heterogeneities can produce two-dimensional flow of meltwater under unsaturated conditions. Finally, it is demonstrated that various assumptions related to density and porosity variations, dimensionality of flow, capillary effects, etc., which have been made by past investigators for ideal situations may not be valid under many circumstances, and several suggestions are made for improving predictions of meltwater behavior. Sensitivity analysis showed that the model is most sensitive to changes in bulk density, residual saturation of wet snow and meltwater supply rates, whereas changes in snow temperature and mean grain size had less marked effect.

INTRODUCTION

Most of the land ice on Earth is below freezing in temperature. In many of these areas the "greenhouse effect" will cause the inception of melting, or increased melting, at the surface. The meltwater, however, will percolate into subfreezing snow and refreeze, releasing latent heat and warming the snowpack. Eventually, the snowpack will be warmed to 0°C, and meltwater can move through the system and into the global ocean, causing sea level rise. Sea level, averaged over the globe, has been rising 1–2 mm/yr during the last 100 years [e.g., *Barnett*, 1984] and is probably caused by a combination of thermal expansion of ocean water and the wastage of glaciers and ice caps on land [*Gornitz et al.*, 1982; *Meier*, 1984; *Barnett*, 1984; *National Research Council*, 1985]. The time scale for contribution of land ice depends on several critical factors, including the speed at which infiltration/refreezing can operate in a vertical (one dimensional) flow system, and to what extent the refreezing process will develop dense, icy layers that will cause lateral movement of meltwater. These issues are not trivial with respect to the timing of global sea level rise: if increased meltwater must penetrate vertically through cold glaciers and ice caps before it can escape to the sea, the time lag between increased melting and sea level rise would be measured in centuries or millennia; if appreciable lateral flow patterns are developed through the growth of icy layers, the time scale could be years or decades.

Attempts to estimate this increasing global sea level range over wide limits (e.g., 0.56–3.45 m by the year 2100 [*Environmental Protection Agency*, 1983]). The wide range of predictions of possible sea level rise reflects a great deal of uncertainty regarding the particular sources for new liquid water, and the physical causes related to each source. In order to reduce this uncertainty, a better understanding of the physical processes which occur when liquid water infiltrates subfreezing snow is needed. Specifically, the process by which the meltwater is transmitted out of the pack to become runoff needs to be investigated in detail [*Dozier*, 1987]. As yet, little progress has been made in developing a comprehensive treatment of the subject, because the combination of liquid infiltration, heat conduction and refreezing of meltwater makes the process difficult to model. A complete consideration of the problem should account for all of the influences which affect the transport of meltwater. Thus the case of subfreezing snow must be studied, so that the process by which the snow reaches thermal equilibrium can be evaluated. Also, spatial heterogeneities and their effects must be considered. Next, capillary effects must be included, since they may have a significant influence on flow at very low saturations or when encountering layers with sharply contrasting densities. Finally, changes in the hydraulic and thermal properties of the snow during the melt, and due to refreezing of meltwater, must be considered.

Only a limited treatment of the process of refreezing of meltwater or the factors which govern it can be found in literature. Most investigators assume an isothermal pack at 0°C [e.g., *Colbeck*, 1974, 1975, 1978, 1979; *Colbeck and Anderson*, 1982; *Ambach et al.*, 1981; *Jordan*, 1983*a*, *b*]. An empirical approach to refreezing is appropriate in many situations, where a rule governing refreezing is used, based on general qualitative or semiquantitative statements about the factors which influence the refreezing of meltwater [*Bengtsson*, 1982; *Marsh*, 1982; *Marsh and Woo*, 1984*a*, *b*]. In these analyses a downward propagation region of isothermal snow containing liquid water is assumed to be separated from dry subfreezing snow along a sharp, moving boundary. The geometry of the boundary is generally a horizontal plane, but *Marsh and Woo* [1984*a*, *b*] adopted a more

Paper number 89WR03170.
0043-1397/90/89WR-03170$05.00

complex front geometry characterized by two depths, or fronts: a depth at which all snow is isothermal (a "background" front) and a lower depth which marks the deepest penetration of isolated incursions of meltwater (a "finger front"). *Marsh* [1982] assumes that all meltwater at the surface will reach the front the same day. *Bengtsson* [1982], on the other hand, includes an implicit finite difference model to route water to the front but offers few details. Furthermore, it is not specified what conditions the assumptions about the requirements for front advancement are valid.

Heterogeneities, which can cause uneven wetting (and warming) of the snowpack, provide some of the motivation for a two- or three-dimensional modeling approach. The first to attempt to address this problem was *Colbeck* [1975]. Because of a "lack of quantitative knowledge of snowpack stratigraphy," *Colbeck* [1975, p. 261] suggests that an equivalent homogeneous anisotropic porous medium be used to model the effect of layered heterogeneities. *Marsh and Woo* [1985] noted that there is horizontal flow due to semi-impermeable ice layers sometimes scattered throughout in the snowpack. Because these ice layers are slightly porous, water flows through as well as over them. Therefore they suggest a multiple flow path model to imitate this process. Although both of these examples attempt to account for increased travel time of meltwater due to spatial variations, they are still one dimensional in essence.

Among the efforts to actually solve a governing equation of unsaturated flow through snow, two distinct approaches have been taken. The gravity flow theory, applied by *Colbeck* [1974, 1978, 1979] in several papers and later used by others [*Ambach et al.*, 1981; *Marsh and Woo*, 1985], assumes that capillary pressure gradients are unimportant. *Colbeck* [1978] readily admits, however, that capillary gradients are important at lower flow rates and saturations and in highly heterogeneous snow. Considering the relatively low melt rates which may be expected in higher latitudes, it is likely that capillary gradients are quite important in routing meltwater there. *Jordan* [1983*a*, *b*] does incorporate capillary pressure gradients in a finite difference model of meltwater infiltration, but it is for isothermal snow and does not consider phase change or heat transfer. Thus it resembles an unsaturated soil model.

This paper attempts to lay the foundation for a mathematical model which can treat all the important aspects of meltwater flow into and through cold snow. The modeling effort concentrates on understanding the routing of meltwater to the wetting front and the physics which govern the wetting front advance. An understanding of these phenomena and a multidimensional flow model are necessary to analyze such complex phenomena as wetting front instabilities and flow fingers. Structural changes in the snowpack, such as formation of ice layers, are the consequence of a particular pattern of meltwater routing in the snow together with boundary conditions which dictate the temporal pattern of overall warming and cooling. We investigate here the ways in which water is concentrated to form layers. The model in its present form does not incorporate several important phenomena such as grain growth and compaction which occur in the wet zone behind the front. These have significant effects on water routing to the wetting front and have been analyzed by *Colbeck* [1973]. They are being included in the new generation of models which are currently under development.

Because of the spatial variability and temperature and time dependence of hydraulic properties of the snow, a numerical model is necessary to simulate the water and heat flow processes in snow. Because the spatial variability of parameters occurs over relatively short distances, the computer memory requirements and the number of computations are substantial. Thus for longer simulations a supercomputer with vector processing capabilities was used. A sensitivity analysis shows the relative importance of changes in values of various input data. The results of these analyses were used in the design of the field data collection currently in progress at Ellesmere Island in Arctic Canada.

MATHEMATICAL MODEL

In order to model meltwater infiltration in subfreezing snow, three major processes must be considered: water flow through a porous medium under partially saturated conditions, refreezing of meltwater in subfreezing snow, and heat conduction.

Water Flow in Snow

Snow cannot be treated as a classical porous medium. Because there may be heat transfer between the liquid and the solid, resulting in phase changes, the hydraulic properties of the medium are not conservative. However, at any given instant during the melting and refreezing process the various parameters which are used to define its hydraulic characteristics can be determined. Before formulating the fluid flow problem, it is useful to discuss briefly some of the specific qualities of snow as a porous medium. Relevant issues include snow heterogeneity and grain structure and how they affect the storage and flow parameters of snow.

Gerdel [1954] investigated the effects of macroscopic layering and smaller-scale spatial variations in bulk density and grain structure on the flow of meltwater. From snow pit experiments he noted that in rapidly melting snow, preferred flow channels developed, both in the horizontal and vertical directions. *Marsh* [1982] and *Marsh and Woo* [1984*a*] confirmed these phenomena. The layering results primarily from the differences in the meteorological events which deposit each layer. *Marsh* [1982], who studied snowpacks in northern Canada, noted that these layers are usually homogeneous in the macroscopic scale.

Colbeck [1986] stresses the importance of recognizing that wet and dry snow act as two distinct substances. At lower temperatures, especially at higher temperature gradients, the equilibrium shape of an ice crystal in air is faceted. At higher temperatures the equilibrium form is well rounded [*Colbeck*, 1983]. Once water is introduced to dry snow which is highly faceted, rapid metamorphism occurs, and the grain becomes well rounded "almost instantly" [*Colbeck*, 1978, p. 171]. If the snow is wet for a significant amount of time, larger grains will grow at the expense of smaller ones, resulting in an increase in the mean grain size and a consequent increase in permeability of the wet snow [*Colbeck*, 1983].

The governing equation for two-dimensional (in a vertical plane) unsaturated flow in a porous medium, derived from Darcy's Law and the equation of continuity, is given by *Corey* [1986]:

$$\frac{\partial}{\partial x}\left[Kk_{rw}\left(\frac{\partial \psi}{\partial x}\right)\right]+\frac{\partial}{\partial z}\left[Kk_{rw}\left(\frac{\partial \psi}{\partial z}+1\right)\right]+Q=C\frac{\partial \psi}{\partial t} \quad (1)$$

where K is the saturated hydraulic conductivity, k_{rw} is the relative permeability of water at a given saturation, ψ is the pore water pressure head, Q is a positive liquid flux into the system, C is the moisture capacity, and the x and z are the horizontal and vertical axes, respectively. The saturated hydraulic conductivity is defined as

$$K=\frac{k\rho_w g}{\mu_w} \quad (2)$$

where k is the intrinsic permeability, ρ_w is the density of water, and μ_w is the viscosity of water. The moisture capacity is defined as

$$C=\phi\frac{\partial S}{\partial \psi} \quad (3)$$

where S is the water saturation and ϕ is the porosity. Because the relative permeability, k_{rw}, is a function of saturation, and saturation is in turn a function of pore water pressure, (1) is nonlinear. In order to solve this equation, the intrinsic permeability as well as the functional relationships between relative permeability and saturation and between saturation and pressure head have to be known. The expression most often used to calculate the intrinsic permeability, k, of snow was developed empirically by *Shimizu* [1970]:

$$k=0.077\,d^2\exp(-7.8\rho_s) \quad (4)$$

where d is the mean grain size, and ρ_s is the bulk density of the snow. It was developed for snow grains of less than 1.0 mm grain size, but *Colbeck* [1978] suggests that it is reasonable to apply it to grains up to 2.0 mm. Nearly all attempts to model the flow of water in snow which employ an empirical calculation of intrinsic permeability (rather than a direct measurement) have used (4) [e.g., *Ambach et al.*, 1981; *Jordan*, 1983*a*, *b*]. It should be stressed, however, that its validity has not been well substantiated for snow which has been subjected to a great deal of meltwater refreezing.

The relationship between saturation and pressure head is usually presented in terms of the effective saturation. The effective saturation is defined as

$$S_e=\frac{S-S_r}{1-S_r} \quad (5)$$

where S_e is the effective saturation and S_r is the residual saturation. For wet snow at 0°C, *Colbeck and Anderson* [1982] determined S_r to be 0.07, *Bengtsson* [1982] found it to be 0.05, whereas *Ambach et al.* [1981] chose a value of 0.03. The pressure above which a porous medium becomes saturated is called the "air entry pressure," ψ_a. The Brooks-Corey expression [*Corey*, 1986], commonly used to relate effective saturation, S_e, to the pore water pressure head, ψ, is written as follows:

$$S_e=\left(\frac{\psi_a}{\psi}\right)^{\lambda} \quad (6)$$

for $\psi<\psi_a$ and

$$S_e=1.0 \quad (7)$$

for $\psi\geq\psi_a$. The variable λ characterizes the pore size distribution [*Corey*, 1986]. For snow, *Wankiewicz* [1979] determined ψ_a to be between −30 mm and −40 mm head of water, and for drainage, he determined λ to be 4. *Jordan* [1983*a*] concurred with this range for ψ_a, but he stresses that for wetting, a better value for λ is 2. It remains unclear how such factors as porosity, mean grain size, and past melt/freeze events affect this curve.

Relative permeability has traditionally been written as an empirical power function of effective saturation [*Corey*, 1986]

$$k_{rw}=S_e^{\varepsilon} \quad (8)$$

The constant ε, unique to the particular combination of fluid and porous medium, is called the "soil index." *Wankiewicz* [1979] suggests a value of 3.3–3.5 for ε, whereas *Colbeck and Anderson* [1982] and *Jordon* [1983*b*] suggest using an integer value of 3.

Refreezing of Meltwater

The following is offered as a useful empirical method of approximating the process of meltwater refreezing, based on a few physical properties of the snow grains.

The total amount of energy H which is required to bring a unit volume of snow, with bulk density ρ_s, and subfreezing temperature T to 0°C is

$$H=-\rho_s C_i T \quad (9)$$

where C_i is the heat capacity of ice. The energy released per unit mass of water that freezes is simply its latent heat of fusion, or L. If all the latent heat associated with freezing is utilized in raising the temperature of snow from subfreezing temperature T to 0°C, the maximum mass of water that can be frozen by a unit volume of snow, $m_{\max}$, is equal to the mass which must freeze to raise the snow temperature to zero. To satisfy conservation of heat, the following relation holds:

$$Lm_{\max}=-\rho_s C_i T \quad (10)$$

Equation (10) presupposes that the freezing process is allowed sufficient time to reach completion. In general, the time steps used in modeling will be small in comparison. Therefore in a given modeling step, only a fraction of the potential mass will freeze. Thus the real mass of water, m, which freezes per unit volume of snow in a given increment of time can be expressed as a fraction of potential maximum mass, given by

$$m=fm_{\max} \quad (11)$$

where f is a real number between 0 and 1.

In order for meltwater to refreeze, the snow must absorb heat energy from the water. On the microscopic level, the surface of grains in contact with liquid water can be assumed to be at or near freezing, whereas the center of the grains is colder. As freezing occurs, the latent heat released by the water must be conducted toward the center of the grain, thus raising the temperature of the snow grain. Physical parameters which influence this phenomenon include the thermal conductivity of ice and the snow grain structure.

Another consideration is the area of contact between the snow grain and the liquid water. The greater the surface area of contact, the greater will be the bulk transfer of heat to the grain. *Colbeck* [1978] states that even at infiltration rates as high as 3.0 mm per hour, saturation never gets much larger than about 10%. At smaller melt rates, variations in the total surface area of the snow particles should not appreciably affect the freezing rate.

In order to approximate f, which determines the actual mass of water which freezes as a fraction of the maximum potential mass of water in a small finite time step, a macroscopic parameter, C_k, is introduced. This "freezing calibration constant" incorporates the thermal conductivity of the snow grains and the effects of their shape and size. It is assumed that f is directly proportional to the time step, Δt, and to C_k, or

$$f = \Delta t C_k \tag{12}$$

Thus

$$m = m_{\max} \Delta t C_k \tag{13}$$

Note that for f to be dimensionless, C_k must have units t^{-1}, which indicates that it is a measure of the rate of heat transfer. Until a physically based approach is developed to quantify this parameter based on snow characteristics, C_k is treated as a macroscopic calibration parameter.

Because of the refreezing meltwater, several characteristic parameters of the snow are altered. The new value of porosity at the end time step Δt due to freezing of water in the pores is calculated as

$$\phi^{t+\Delta t} = \phi^t + \frac{m}{\rho_i} \tag{14}$$

where ϕ^t and $\phi^{t+\Delta t}$ are the porosities at the beginning and end of time step Δt, respectively; m is the mass frozen per unit volume, and ρ_i is the density of ice. From the new porosity and the remaining unfrozen water content, the new saturation is calculated as

$$S^{t+\Delta t} = \frac{\theta^t - v_f}{\phi^{t+\Delta t}} \tag{15}$$

where θ^t is the volumetric water content before freezing, and v_f is the volume of water which freezes per unit volume of snow. From this new saturation and the saturation versus pressure curve, a new pressure can be assigned. The new bulk density, $\rho^{t+\Delta t}$, is

$$\rho^{t+\Delta t} = \rho^t + m \tag{16}$$

where ρ^t is the bulk density at the beginning of the time step. From the new bulk density a new intrinsic permeability is assigned according to the *Shimizu* [1970] expression given in (4).

Strictly speaking, because refrozen meltwater becomes attached to existing snow grains, the mean grain size should be updated as well, and its new value should be used in the reevaluation of permeability. However, the *Shimizu* [1970] expression for permeability as given by (4) is significantly more sensitive to change in bulk density than to the change in mean grain size. The process of updating the mean grain size would be difficult to model. Ice grains may become cemented together by new ice, making it difficult to define a new grain size.

Finally, in computing the new temperature the latent heat released from freezing and absorbed by the snow has to be taken into consideration. For convenience in modeling it is assumed that the time step is sufficiently small that the latent heat generated during the current time step is utilized in raising the snow temperature in the next time step. Thus since the total heat energy is conserved, the new temperature at the end of time step Δt, can be computed by

$$T^{t+\Delta t} = \frac{\rho^t C_i T^t + mL}{\rho^{t+\Delta t} C_i} \tag{17}$$

where T^t and $T^{t+\Delta t}$ are the temperature at the beginning and end of the time period, respectively.

Heat Conduction in Snow

Because snow is not a continuous solid material, but a matrix made of ice grains and pore spaces filled with air and vapor, a classical thermal conductivity cannot be defined. In snow, heat is transferred not only by conduction though ice grains but also through convection and radiation across the pores and by vapor diffusion. For this reason an "effective thermal conductivity" is used instead. An approximate graphical representation of the relation between snow density and effective thermal conductivity is suggested [*Male and Gray*, 1981, p. 297]. Expressed functionally, the graph can be summarized as follows: for snow with bulk density, ρ_s less than or equal to 0.45 Mg m^{-3}, the effective thermal conductivity, k_e, is

$$k_e = 0.307\rho_s + 1.964\rho_s^2 \tag{18}$$

where k_e is in W m^{-1} °C^{-1}. For bulk density greater than 0.45 Mg m^{-3},

$$k_e = 2.98\rho_s - 0.805 \tag{19}$$

The governing equation for two-dimensional, transient heat conduction is [e.g., *Ozisik*, 1980]

$$\frac{\partial}{\partial x}\left(k_e \frac{\partial T}{\partial x}\right) + \frac{\partial}{\partial z}\left(k_e \frac{\partial T}{\partial z}\right) = \rho_s C_i \frac{\partial T}{\partial t} + Q_h \tag{20}$$

where x and z are orthogonal axes, T is temperature, k_e is effective thermal conductivity, ρ_s is bulk density of snow, C_i is the heat capacity of ice, t is time, and Q_h is a source or sink term. The latent heat released from meltwater refreezing has already been accounted for in the adjustment of local temperatures. Therefore since there is no other flux of heat into the system, the source/sink term Q_h becomes zero.

In order to solve this equation, the temperature and the bulk density of the snow must be known everywhere. The heat capacity of ice is regarded as a constant, and the effective thermal conductivity is computed from the bulk density.

NUMERICAL MODEL DESIGN

Modeling the transport of fluid and heat in snow is complex, especially because of the nonlinear and implicit nature of the problem. Liquid flow, meltwater refreezing and heat conduction occur simultaneously. In spite of this, if the

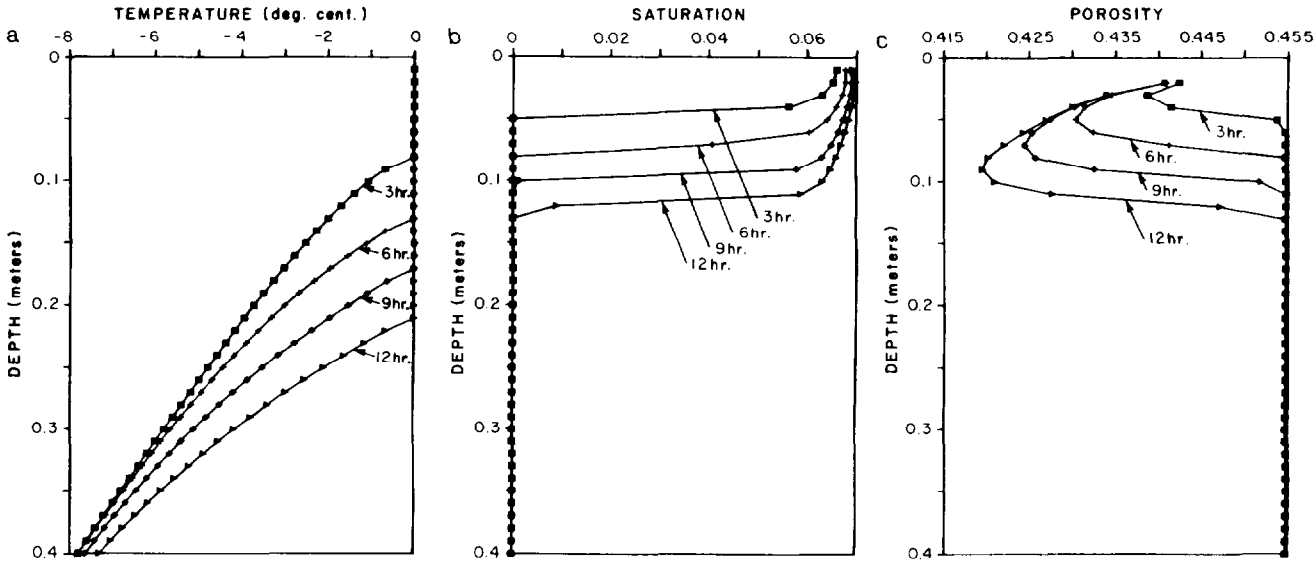

Fig. 1. Simulated profiles of snow properties versus depth for an infiltration rate of 0.5 mm h^{-1}: (*a*) temperature versus depth, (*b*) saturation versus depth, and (*c*) porosity versus depth.

time steps are sufficiently small, an explicit coupling between the fluid flow, phase change and heat transfer can be used. In the numerical model discussed here, this explicit coupling method is employed.

First, a finite element model of unsaturated flow through porous media is executed using relatively short time steps. The element sizes and lengths of time steps used in the various test simulations will be given later. Second, meltwater refreezing is determined as described before. The volumetric water content for the element is computed as an average of the values at its nodes. From the water content of each element and its temperature, the mass which freezes is calculated according to (10) and (13). Then the porosity, bulk density, saturation, and temperature are updated according to (14)–(17), and the new permeability is computed from (4). From the new saturation the new capillary pressure is assigned based on the capillary pressure versus effective saturation relationship. Last, the finite difference heat conduction routine is superimposed over the fluid transport model for the same time step, taking as its initial conditions and thermal properties those which are generated by the freezing routine. The finite element variably saturated flow model, UNSAT2 [*U.S. Nuclear Regulatory Commission*, 1983], was chosen not only as the unsaturated flow module but also as the main shell of the snowmelt program. In order to make it useful for the modeling of snow, several modifications had to be made. These included the removal of various options of the program which were not used in this application, and the simplification of the input data. Furthermore, some code was rewritten to take advantage of the vectorizing compiler on the Cyber 205 supercomputer.

The data necessary to run the snowmelt program include the initial bulk density, mean grain size, and temperature of each element, fluid and heat boundary conditions, parameters which define the characteristic curves of the snow, and the freezing calibration constant. Details of the program input are given in a program user's manual [*Walter and Illangasekare*, 1988].

MODEL APPLICATION

Various simulations were performed with the numerical model. First is a series of two one-dimensional simulations, which show in the simplest possible geometry that the model qualitatively produces results which are expected for two infiltration rates. Then a sensitivity analysis is performed for a vertical infiltration problem, to determine the model sensitivity to each of its inputs. It also serves to help establish how accurately different data should be measured in the field to design the field experiments. Furthermore, it can also shed light on the significance of certain assumptions of the model. Next a series of simple two-dimensional tests is presented, again to show that the model qualitatively produces expected results. Finally, a couple of comparatively larger, more complex two-dimensional simulations are performed, in order to compare the model's performance on a conventional computer and on a vector-processing supercomputer.

One-Dimensional Simulations

For the first two one-dimensional simulations an initially homogeneous domain 0.5 m in depth was used. The initial uniform bulk density was 0.5 Mg m^{-3}. The initial temperature was a linear distribution with 0.0°C at the top and −10.0°C at a depth of 0.5 m. The residual saturation was 0.05. Two infiltration rates (or melt rates) of 0.5 mm/h and 1.0 mm/h, respectively, were simulated for 12.0 hours. Time steps varying from initial value of 0.02 hour to a maximum of 0.10 hour were used. A constant element size of 0.01 m was used throughout the depth of the sample. The freezing calibration constant, C_k, was set such that during each step all of the water present which could potentially be frozen would freeze. The results are summarized in Figures 1 and 2, which show temperature, saturation and porosity as a function of depth at 3.0-hour increments for the two infiltration rates.

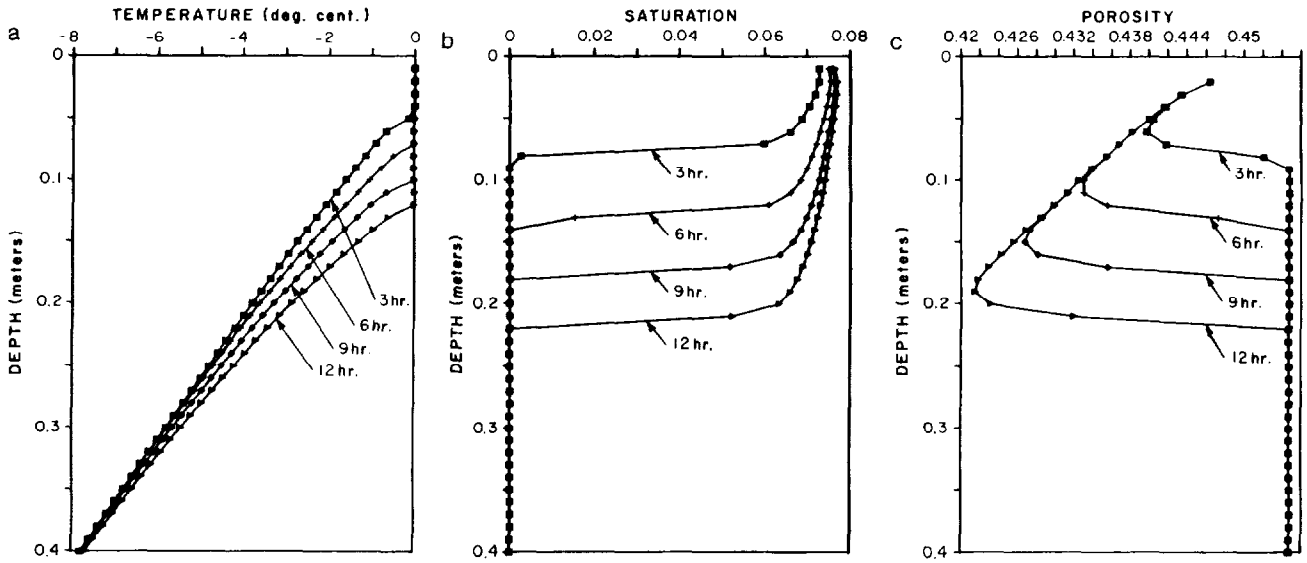

Fig. 2. Simulated profiles of snow properties versus depth for an infiltration rate of 1.0 mm h^{-1}: (*a*) temperature versus depth, (*b*) saturation versus depth, and (*c*) porosity versus depth.

The temperature-depth profiles in Figures 1*a* and 2*a* show that a 0°C isotherm is propagating downward with time. Also it is seen that as the infiltration rate increases the isotherm penetrates faster and deeper into the cold snow. The saturation-depth profiles (Figures 1*b* and 2*b*) also show a front separating wet and dry snow which is propagating downward. Note that at any given depth, saturation remains zero until the temperature there reaches melting. Then the saturation continues to rise, even above the residual value of 0.05, until its relative permeability is sufficient to pass a significant amount of water to the element below, soon after which the saturation reaches an approximate steady state.

The porosity-depth profiles (Figures 1*c* and 2*c*) are consistent with that of temperature and saturation. Comparing the porosity profiles with the saturation profiles shows that for each time, at the depth at which the snow has just become wet, the porosity has begun decreasing appreciably, due to the refrozen water. Then, after the element reaches 0°C, the freezing ceases and the porosity remains constant. The porosity attained a constant value as the model assumes that there is no snow compaction and that grain growth does not occur. Because the deeper snow is colder, more water must freeze to warm it to 0°C. For this reason, the porosity change is greater with depth.

Sensitivity Analysis

Using the previous example with an infiltration rate of 1.0 mm/h as a reference for comparison, a sensitivity analysis was performed by holding all but one of the parameters constant. Each variable tested was adjusted to determine sensitivity of the model outputs to changes in input. The variables chosen were mean grain size, snow bulk density, temperature boundary conditions and residual saturation. The first two tests evaluate the model sensitivity to changes in mean grain size d. Simulations were conducted for mean grain sizes of 0.5 mm and 0.2 mm, respectively. These correspond to a 50% and a 80%, respectively, reduction in grain size from the reference. In the third test all the parameters were maintained at the same values as in the reference run except the snow bulk density, ρ_s, was increased by 20%, changing from 0.5 Mg m^{-3} to 0.6 Mg m^{-3}. The fourth test was performed to evaluate the sensitivity of the bottom temperature boundary condition. The boundary temperature was reduced to −15°C, still maintaining initial temperature distribution linear between the top and the bottom of the snow column. The last test is for a 20% reduction in the residual saturation, S_r, from the reference value of 0.05 to 0.04. The combination of values of the input

TABLE 1. Data for One-Dimensional Sensitivity Analysis

Test	Grain Size d, mm	Density ρ_s, Mg/m^3	Bottom Temperature, °C	Residual Water Content S_r
Reference	1.0	0.5	−10.0	0.05
1	0.5	0.5	−10.0	0.05
2	0.2	0.5	−10.0	0.05
3	1.0	0.6	−10.0	0.05
4	1.0	0.5	−15.0	0.05
5	1.0	0.5	−10.0	0.04

TABLE 2. One-Dimensional Sensitivity Analysis Results

Test	Front Depth at 6 Hours, z_6, cm	Front Depth at 12 Hours, z_{12}, cm	Maximum Porosity Change $\Delta\phi_{max}$	Maximum Saturation S_{max}
Reference	13	21	0.0332	0.0771
1	12	20	0.0332	0.0891
2	11	19	0.0299	0.0951
3	19	23	0.0455	0.0806
4	14	21	0.0368	0.0735
5	14	24	0.0343	0.0654

variables used in the reference run and each of the tests are summarized in Table 1.

Table 2 summarizes the results of the sensitivity analysis from the five test simulations as compared to the reference run. Four output variables were selected to evaluate the model sensitivity, namely, the front depth at 6.0 hours, z_6, the front depth at 12.0 hours, z_{12}, the maximum change of porosity in the domain at 12.0 hours, $\Delta\phi_{max}$, and the maximum saturation in the solution domain, S_{max}.

The tests on grain size sensitivity (tests 1 and 2) showed that the maximum porosity changes are practically identical to those generated in the reference test with 1.0 mm grains, because the densities and temperatures have not changed. Because the flux input is the same, but the intrinsic permeability has decreased, the saturations are slightly larger. These higher saturations, in turn, result in a higher relative permeability. Because of the higher relative permeability, the reduction of intrinsic permeability does not have the effect which might be expected. In fact the depth of propagation at 1.20 hours for test 2 is only reduced by 2.0 cm (about 10%) even with a mean grain size of 0.2 mm.

The results of the bulk density test (test 3) are discussed next. Because the density is larger, and the initial temperature is the same, more latent heat is required to bring the snow to the freezing point, so more water must freeze. Thus as expected the maximum change in porosity due to refreezing is correspondingly larger. Because of the increase of water frozen, one might expect that the wetting front would not propagate as deep into the snow. In reality however, it propagates deeper. Because the porosity of the snow is smaller than before, a smaller volume of water is required in order to bring the saturation up to residual, thus allowing the water to infiltrate farther and faster. Once again, because the large density reduces the permeability, but the flux is the same, the saturations are correspondingly larger.

In test 4, with the lower temperature boundary at −15.0°C, since the colder snow requires more latent heat to bring it to melting point, the maximum change in porosity is more than that of the less cold snow. However, little change in the wetting front depth occurs as a result of the lower temperatures. At this infiltration rate the mass of water required to freeze per unit volume to raise the temperature by 5.0° is small compared to the total mass of water added to the system. Note that even though the initial hydraulic parameters are the same for both the reference run and this test, the maximum saturation of the colder snow is slightly higher, because the greater refreezing results in a lower porosity.

Finally, in test 5 with reduced residual saturation, little variation from the reference run is seen in the maximum porosity change due to freezing. However, two important changes are noticed as a result of the lower residual saturation. First, the maximum saturation is correspondingly lower. Second, because less water is required to bring a unit volume of dry snow up to residual saturation, the wetting front propagates farther and faster.

From the analysis described above, it is clear that the input variable which must be measured most accurately is the bulk density of the snow, as small variations in it result in significant changes in the speed of the propagation of the wetting front. Next in order of importance is the residual saturation. Even a 20% error in its measurement has a significant effect in the calculated wetting front depth. It should be remembered that an assumption of the numerical model is that the residual saturation of the snow is constant everywhere and does not vary with density. If this is not true in nature, significant error could result if adjustments to the model are not made. An error in the temperature of the snow of 5.0° seems to have little effect. Finally, it has been shown that at least for snow with bulk density larger than 0.5 Mg m^{-3} even an 80% error in the mean grain size results in little change in the wetting front advancement.

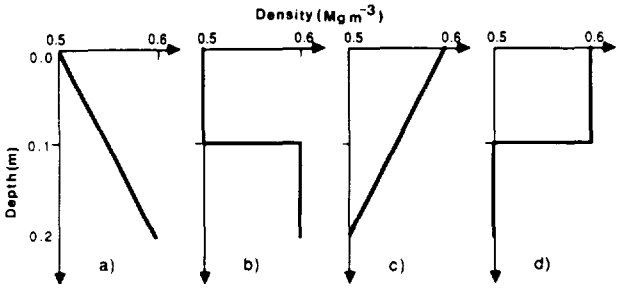

Fig. 3. Initial density profiles for four different layered density simulations: (*a*) gradual increase, (*b*) sudden increase, (*c*) gradual decrease, and (*d*) sudden decrease.

Density Discontinuities

The next set of test simulations was conducted to study the effect of layered density variations on the water infiltration and front propagation. For all the simulations which follow, the infiltration rate is kept uniform at 1.0 mm/h across the top of the snow column. Also, the residual saturation is 0.05, and the initial temperature decreases with depth from 0.0°C, at the top, at a rate of 0.2°C/cm. Finally, unless otherwise noted, the grain size is always kept at 1.0 mm.

Jordan [1983*a*] and others suggest that density variations may play an important role in the transfer of water and heat. To this end, four tests were devised to examine the influence of density variations within the snowpack. Each of them represents some type of density variation within the uppermost 20.0 cm of snow. The initial density profiles of each is depicted in Figure 3.

The results of the four test simulations are summarized in Table 3. It shows the depth of the wetting front at 2.0, 4.0, 6.0 and 8.0 hours, or z_2, z_4, z_6 and z_8, respectively. The snow which increases in density with depth slows the wetting front down as it gets deeper. On the other hand, in the snow which decreases in density with depth, the wetting front travels at an approximately constant rate. Another interesting result is that whether the density variation is

TABLE 3. Results From the Test Runs on Density Variations

Density Distribution	Front Depth at 2 Hours, z_2, cm	Front Depth at 4 Hours, z_4, cm	Front Depth at 6 Hours, z_6, cm	Front Depth at 8 Hours, z_8, cm
Gradual increase	5	9	12	14
Sudden increase	5	10	12	14
Gradual decrease	6	11	15	20
Sudden decrease	6	11	15	20

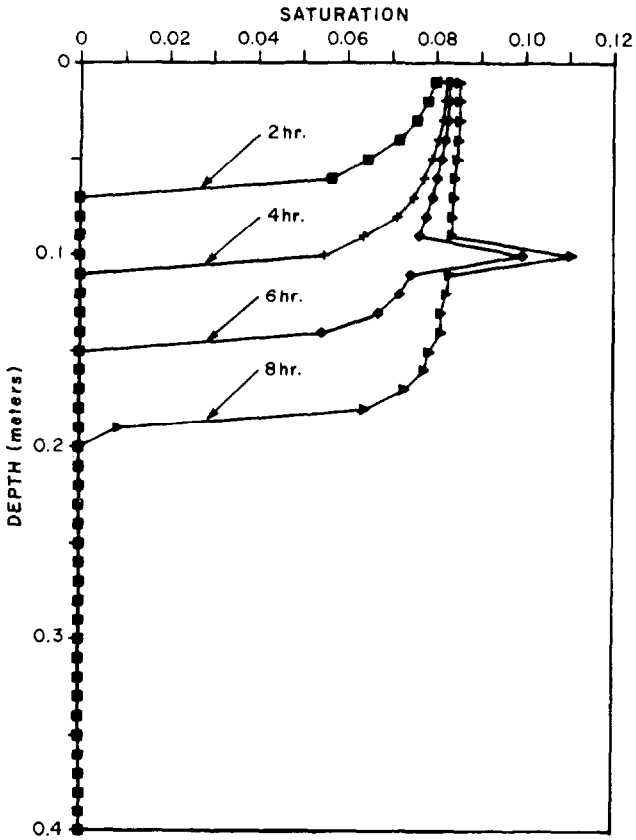

Fig. 4. Simulated saturation profiles for an abrupt drop in density.

gradual or sudden has little influence on the final wetting front depth or its average speed.

The saturation profiles of the abrupt decrease in density merit a closer look. As shown in Figure 4, an interesting occurrence can be seen when the wetting front reaches the interface between the two layers of differing density. In the deepest element of the more dense layer, just above the less dense layer, the saturation is significantly larger than everywhere else. Thus a significant portion of the water which has entered the system is "hanging" on the bottom of this more dense layer rather than passing down into the layer below. In the upper layer, which has a smaller porosity, the saturation is higher, resulting in a higher relative permeability than the layer below. Thus the water flows to the interface between the layers relatively quickly. However, when it reaches the less dense snow, which has a greater porosity, the relative permeability is smaller. This causes the water to slow down, resulting in the buildup of liquid in the lowest element of the more dense layer. This suggests that differences in relative permeability as well as capillary gradients may affect flow at the interface between layers of varying density.

The behavior predicted in Figure 4 can also be observed in the field. Figure 5 summarizes the author's observations in Arctic Canada of this phenomenon. The snow stratigraphy at a site on the summit of Mer de Glace Agassiz, Ellesmere Island, was measured in 1988 and 1989. Figure 5 shows the profiles of density in the near-surface layers. The features of interest are the development of ice layers on top of three depths hoar layers in the 1988 accumulation, at depths in the 1989 stratigraphy of 17 cm (May 1988, surface), 34 cm (A/B horizon) and 48 cm (C/D horizon).

In the 1988 stratigraphy, layers B and D were well-developed depth hoar layers, with faceted, angular grains 1–3 mm in diameter. These layers were generally 1–3 cm in thickness and were very continuous over distances of several hundred meters. In the 1989 stratigraphy, layers B and D still contained faceted grains but with some alteration by melt/freeze metamorphism (referred to as "iced depth hoar"). Similarly altered depth hoar, capped by a thin ice layer, was present above the May 1988 surface. This was depth hoar presumably developed before the onset of the 1988 melt season. Automated measurements during summer of 1988 recorded snowfall in June, before the onset of the meltwater season in July. This snowfall corresponds to the layer between the 1988 summer surface and 1988 May surface in the 1989 stratigraphy, where meltwater alteration was present in May 1989.

Ice layers in more than 15 pits logged in 1988 and 1989 were almost invariably found at the upper surface of low density layers (some deeply buried ice layers appeared without low density layers, but at such depths there were generally no low density layers preserved at all). The stratigraphy in Figure 5 shows in particular that the ice layers developed along the preexisting low density layers. Essentially the same pattern of ice layers was created artificially in 1988 by heating the air at the surface of the snow and forcing melting. In this case, the thickest ice layer developed at the C/D horizon, rather than the A/B horizon, as shown in Figure 5. It is interesting to note, however, that in both the artificial and the natural melt situation, the thickest layer developed at the second depth hoar layer below the surface (A/B horizon in May 1988 and C/D horizon in July 1988). The smaller size of the uppermost ice layer in both cases may be because the near-surface snow was warmer (due to meltwater refreezing) and consequently was not sufficiently cold to freeze the wet layer in situ.

Two-Dimensional Simulations

In order to observe the effects of capillary pressure gradients and heterogeneities of snow on water infiltration, simple simulations were performed using idealized two-dimensional density distributions. For each test a domain 0.25 m wide and 0.25 m deep was used. In these simulations the problem domain was discretized into equal sized 1.0 cm × 1 cm square grid elements. Simulation time steps ranging from 0.2 to 0.5 hour were used.

In the first example a horizontal ice layer extends all the way across the domain, except for a small opening in the center as shown in Figure 6. The opening is 3.75 cm from the top, and it is 5.0 cm wide. The initial density of the ice layer is 0.7 Mg m^{-3}. The initial density everywhere else is 0.5 Mg m^{-3}. Figure 6 shows the volumetric water content contours at 4.0 hours. It shows that water has flowed through the opening, after which it spread out due to capillary pressure. The solution appears to be slightly skewed to the left. Due to the numerical approximations, perfect symmetry is impossible. Thus from the beginning, one side of the domain inevitably receives slightly more water than the other. As a result, that side also warms quicker, because more water is available to refreeze and release its latent heat. Similarly, this side reaches residual saturation sooner, allowing water

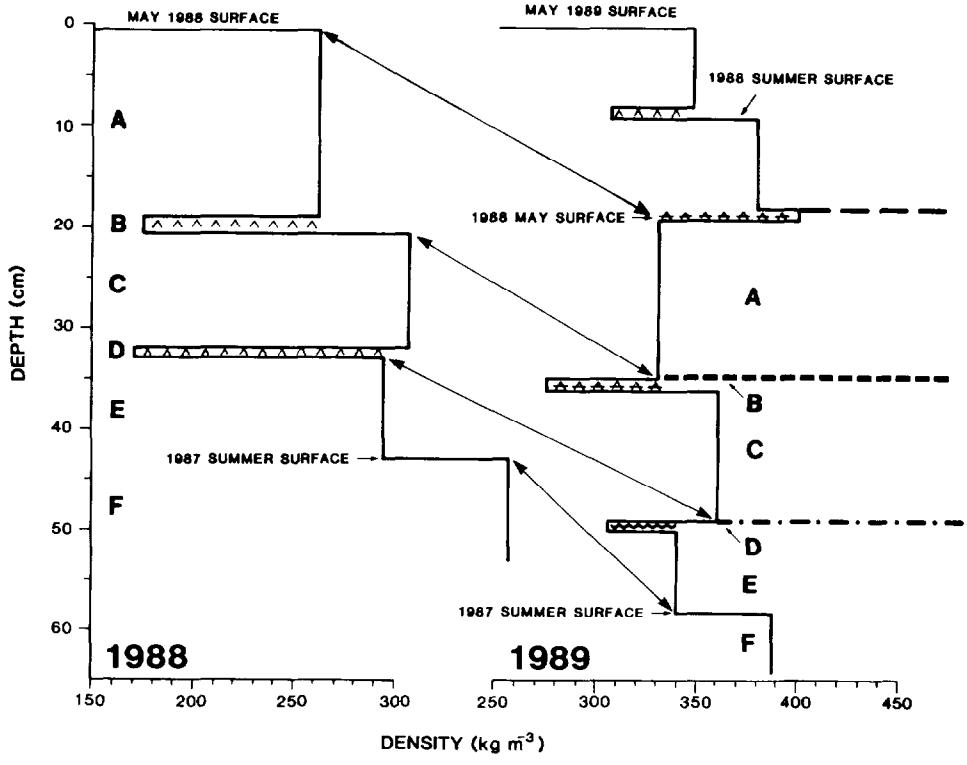

Fig. 5. Profiles of density and snow type in near-surface layers at Mer de Glace Agassiz, Ellesmere Island, Canada, in May 1988 and 1989. The development of ice layers above the low density layers during the summer 1988 melt season is shown. Letters A, B, C, D, E and F denote snow layers defined in 1988 and reidentified in 1989. Snow types are denoted by the following symbols: dashed line, ice layers, dotted dashed line, intermittent ice layers; wavy line, soft layer, upside down V, depth hoar; upside down V with bar, iced depth hoar.

to pass through it sooner. So, the asymmetry is further exacerbated.

Next, to show that the model correctly solves for inclined layering, a simulation of flow with an ice layer sloping to the right was performed. In order to do so, the z axis of the domain was set at a 20.0° angle from the gravity vector. Figure 7 shows the volumetric water content contours at 4.0 hours. It shows, as expected, that water is deterred from flowing through the dense layer. Once past the ice layer, the effects of capillary pressure are clear, as some of the water has actually flowed "uphill." This is shown by the small area of snow under the right corner of the ice layer which has a volumetric water content grater than 0.03. Also, due the slope to the right, the depth of the wetting front increases gradually from left to right.

Complex Two-Dimensional Simulations

Finally, in order to show that the model can accommodate a larger, more complex domain, two more sophisticated simulations were conducted. In both of these runs a domain 0.3 m deep and 0.6 m wide was used. These simulations also provide an opportunity to compare the model's performance on the Cyber 205 supercomputer with that of the VAX/VMS system.

The first of these was for an arbitrary distribution of semi-impermeable layers. The density is 0.7 Mg m^{-3} in each dense layer and 0.5 Mg m^{-3} everywhere else. A slope of 10.0° was assigned to the layers. Figure 8 shows the wetting front at 2.0-hour intervals. It shows clearly that parts of the wetting front are delayed by each semi-impermeable layer. It also shows how capillary pressure causes moisture to be drawn under the ends of each dense layer. Furthermore, this simulation shows that once beyond the last layer the front speeds up slightly. This can be seen from the distance

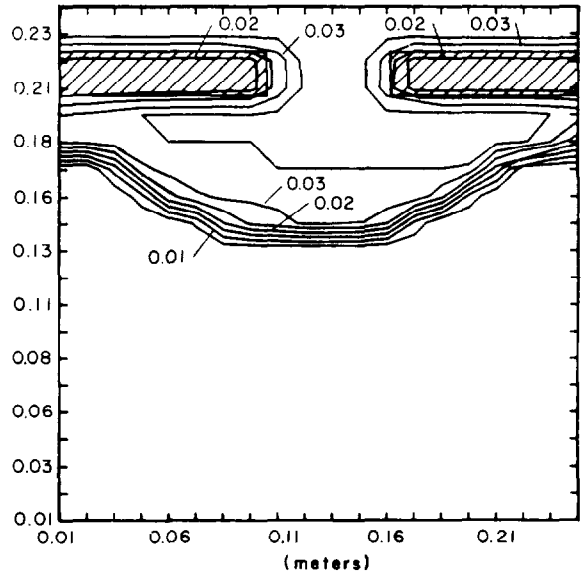

Fig. 6. Volumetric water content contours at 4.0 hours for the center opening example.

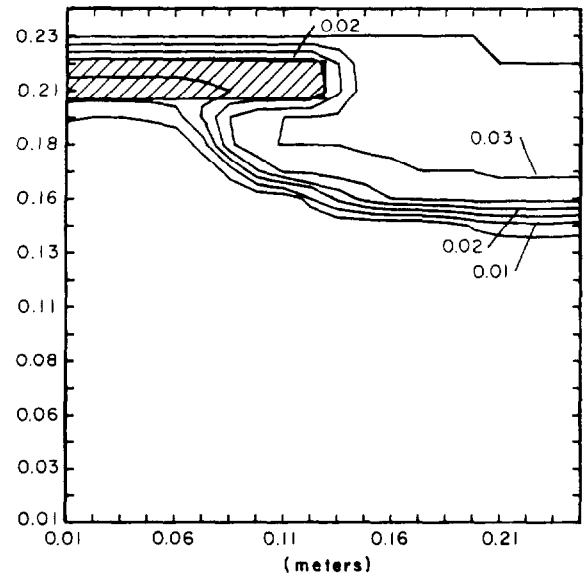

Fig. 7. Volumetric water context contours at 4.0 hours for inclined "ice layer" example.

between the 6.0- and 8.0-hour front lines, compared to the distance between the 4.0- and 6.0-hour front lines.

The next test used the same geometry as the one above. In this case, however, the semi-impermeable layers are replaced with relatively more permeable layers. In order to simulate this, the grain size was set to 3.0 mm in the more permeable layers and 1.0 mm everywhere else. The density of snow is kept at 0.5 Mg m^{-3} everywhere. Since the intrinsic permeability is proportional to the mean grain size squared, the layers are 9.0 times more permeable than the rest of the domain. Figure 9 shows the wetting front at 1.6-hour increments. It shows that as expected parts of the wetting front are accelerated by the more permeable layers. In comparison to Figure 8, one can see that the position of the wetting front is less deep for this case than for the semi-impermeable layers. The reason for this is that the more permeable layers in this simulation have an initial porosity of 0.45, whereas the initial porosity of the semi-impermeable layers in the previous example was 0.23. Therefore the large-grained layers have a considerably greater capacity to store water than the semi-impermeable layers.

For each of the two simulations described above, the VAX CPU time used was approximately 800 s. The CPU time on the Cyber 205, on the other hand, was only 94 s. Thus the supercomputer was over 8 times faster. If a larger domain or a longer simulation is desired, use of the conventional computer will become impractical, and the supercomputer will be necessary. It is expected that the simulations of the field problem will be conducted using the supercomputer.

CONCLUSIONS

This study is an initial attempt to formulate a comprehensive description of the problem of infiltration in cold snow. All of the research which preceded this study made major simplifying assumptions about the process. These included, for instance, one-dimensional flow, isothermal snow, homogeneity, and noncapillary flow. By avoiding these assumptions, this study is expected to more closely approximate the natural processes which influence fluid and heat flow.

A general theory of the processes which control meltwater refreezing was developed, and a freezing calibration constant was defined, which is related to a few simple physical properties. Combining the meltwater refreezing theory and the heat conduction solution with a two-dimensional unsaturated fluid flow model, a comprehensive numerical model of fluid and heat transfer in snow was developed.

Using the numerical model, a sensitivity analysis was used to determine which data must be measured most accurately in the field. This should prove instrumental in the assessment of runoff from cold ice caps caused by a long-term rise in air temperature. It was shown that the model is most sensitive to changes in the bulk density and residual saturation of the snow. Variations in the meltwater supply rate produced a significant change as well. Changes in snow temperature and mean grain size had a less marked effect on the model.

Next, the model was used to study the effects of layered density profiles for sudden and gradual increases or decreases in density. It was demonstrated that gradual changes and sudden changes have approximately the same effect on average speed of propagation. The arrangement of the various layers is significant, however. Saturations are significantly affected by density changes, with regions of high

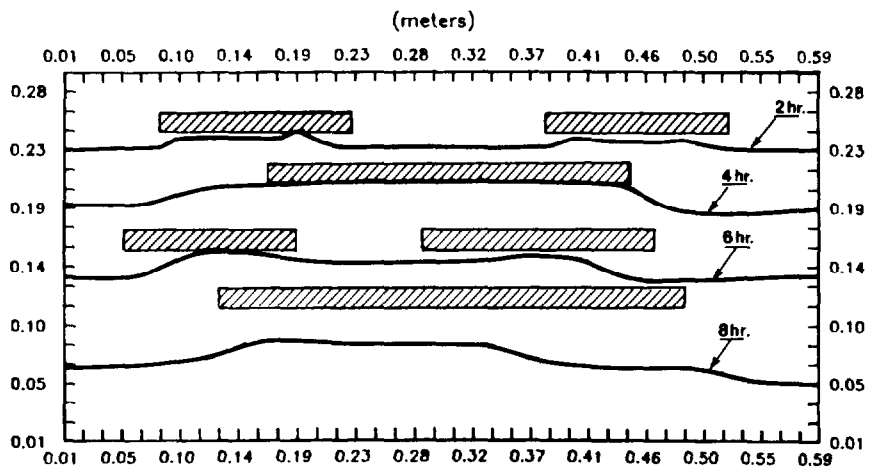

Fig. 8. Wetting front at 2.0-hour increments, for the case of various semi-impermeable layers.

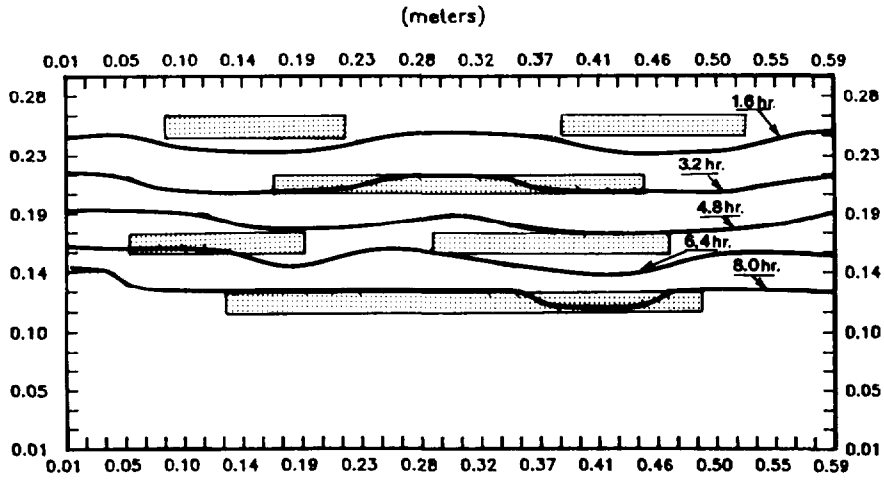

Fig. 9. Wetting front at 1.6-hour increments, for the case of various large-grained materials.

saturation developing at the interface between high-density snow overlaying low-density snow. Therefore it is not sufficient to assign an average permeability to a layered snowpack, because two snowpacks with the same average permeability may behave very differently.

The two-dimensional simulations showed that the model produces a satisfactory simulation of flow over horizontal or inclined semi-impermeable ice layers. It also showed horizontal flow caused by capillary gradients. This was evident in the spreading of the wetting front, after passing through a small opening in an ice layer (Figure 6) and also in the moisture which flowed back uphill after passing over an inclined ice layer (Figure 7).

In order to show that the model was capable of solving larger, more complex systems, the size of the two-dimensional solution domain was increased, and various randomly distributed layers were introduced. These simulations indicate that the model can successfully simulate meltwater movement in a snowpack with layered heterogeneities. Furthermore, it was shown that for longer simulation times and larger solution domains, even the fastest of conventional mainframe computers becomes impractical.

Several nontrivial assumptions led to the development of this model. In order to fully validate it, or to suggest areas where it might be improved, several areas of important research should be investigated.

First of all, it was assumed that both residual saturation and the relationship between capillary pressure and saturation are constant everywhere in the domain. In reality, however, they may be functions of any combination of the following: bulk density, grain size, and grain structure. As was shown in the sensitivity analysis, the model is quite sensitive to errors in the residual saturation, indicating that this issue is a very important one to settle.

Also, more work needs to be done to define the conditions under which the permeability expression is valid. It remains unclear whether it can be accurately applied to a snow sample which has undergone significant refreezing of meltwater, which no longer resembles a granular material. Similarly, the relationship between thermal conductivity and bulk density should be further explored. The developers of the relationship warn that it cannot simply be accepted without verification for a particular type of snowpack. Unfortunately, they offer few criteria for determining its validity for a specific case.

The freezing constant C_k is imposed as a macroscopic calibration constant which represents heat transfer processes on the grain scale which are not considered in the model. Such small-scale processes must not appear explicitly in the model if it is to be used efficiently to predict flow and refreezing on a macroscopic scale, but the grain scale process must be better understood to assign values to C_k with confidence. Until a physically based procedure is developed to estimate the freezing constant, the selection of the length of time step becomes arbitrary. In the examples which were presented earlier, very small time steps were used to allow all the water which could potentially be frozen to freeze. The physical basis of meltwater refreezing must be developed through an analysis of grain scale heat transfer and effects of grain size, shape, initial temperature, and a physical distribution of liquid water. Finally, the freezing calibration constant incorporates implicitly the fact that not all the water introduced into subfreezing snow necessarily freezes in a finite time increment Δt. A more comprehensive treatment of events at the boundary between isothermal snow will include the possibility of an intermediate zone in which liquid water is present in, but not in thermal equilibrium with, subfreezing snow.

The model presented in this paper was designed primarily to conduct analyses to assist us in the development of a field experimental program. The proper field verification of the model requires data on snow-water characteristics for wet snow (relative permeability versus saturation and capillary pressure versus saturation data) and field data on flux rates, temperature profiles, density profiles, snow stratigraphy, etc. To our knowledge no such comprehensive data base exists for conditions in high latitudes. This was the primary purpose of our field data collection program at Ellesmere Island. Our future research efforts are directed toward estimating parameters for snow-water systems in the laboratory and in the field.

Before using the model to estimate the meltwater generation resulting from the greenhouse effect, the model has to be verified in the field. Also, the question of scale effects associated with applying the "point scale" model presented here to regional problems has to be addressed. Both of these

issues will be addressed in an upgraded model which is currently under development specifically for field applications.

NOTATION

C moisture capacity, m^{-1}.
C_i heat capacity of ice, $m^2\ s^{-2}\ °C^{-1}$.
C_k freezing calibration constant, t^{-1}.
d mean grain size of snow, m.
f a real number between 0 and 1.
g gravitational acceleration, $m\ s^{-2}$.
H heat energy required to warm a unit volume of snow to freezing, $kg\ m^{-2}\ s^{-2}$.
K saturated hydraulic conductivity of snow, $m\ h^{-1}$.
k intrinsic permeability of snow, m^2.
k_e effective thermal conductivity, $kg\ m\ s^{-3}$.
k_{rw} relative permeability of snow with respect to water.
L latent heat of fusion of ice, $m^2\ s^{-2}$.
m mass of water frozen per unit volume of snow, $kg\ m^{-3}$.
m_{max} mass of water which must freeze to warm a unit volume of snow to freezing, $kg\ m^{-3}$.
Q liquid flux, $m^3\ h^{-1}$.
Q_h heat flux, $kg\ s^{-2}$.
S saturation.
S_e effective saturation.
S_r residual saturation.
T temperature, 0°C.
t time, s or hours.
v_f volume of water which freezes per unit volume of snow.
ε soil index.
θ volumetric water content.
λ exponent in the S_e expression.
μ_w viscosity of water, $kg\ m^{-1}\ s^{-1}$.
ψ pore water pressure head, mm.
ψ_a air entry pressure head, mm.
ϕ porosity.
ρ_i density of ice, $kg\ m^{-3}$.
ρ_s bulk density of snow, $kg\ m^{-3}$.
ρ_w density of water, $kg\ m^{-3}$.

Acknowledgments. The financial support for this work was provided by the CO_2 Research Division of the U.S. Department of Energy, grant DE-FGO2-87ER60570. Computing support for CYBER 205 at John Von Neumann Center for Scientific Computing at Princeton was through National Science Foundation grant ECS-8515986 through the Office of Advanced Scientific Computing. Both of these funding sources are gratefully acknowledged. The authors wish to thank the anonymous reviewers for their comments which the authors found to be very valuable in revising the paper. Also, we would like to thank Sam Colbeck for his interest in our research and for reviewing some of the ideas presented in this paper.

REFERENCES

Ambach, W., M. Blumthaler, and P. Kirchlechner, Application of the gravity flow theory to the percolation of melt water through firn, *J. Glaciol.*, *27*(95), 67–75, 1981.

Barnett, T. P., The estimation of "global" sea level change: A problem of uniqueness, *J. Geophys. Res.*, *89*(C5), 7980–7988, 1984.

Bengtsson, L., Percolation of meltwater through a snowpack, *Cold Reg. Sci. Technol.*, *6*, 73–81, 1982.

Colbeck, S. C., Theory of metamorphism of wet snow, *Res. Rep. 313*, p. 11, Cold Reg. Res. and Eng. Lab., Hanover, N. H., 1973.

Colbeck, S. C., Water flow through snow overlying an impermeable boundary, *Water Resour. Res.*, *10*(1), 119–123, 1974.

Colbeck, S. C., A theory for water flow through a layered snowpack, *Water Resour. Res.*, *11*(2), 261–266, 1975.

Colbeck, S. C., The physical aspects of water flow through snow, *Adv. Hydroscience*, *11*, 165–206, 1978.

Colbeck, S. C., Water flow through heterogeneous snow, *Cold Reg. Sci. Technol.*, *1*, 37–45, 1979.

Colbeck, S. C., Snow particle morphology in the seasonal snow cover, *Bull. Am. Meteorol. Soc.*, *64*(6), 602–609, 1983.

Colbeck, S. C., Classification of season snow cover crystals, *Water Resour. Res.*, *22*(9), 59S–70S, 1986.

Colbeck, S. C., and E. A. Anderson, Permeability of a melting snowcover, *Water Resour. Res.*, *18*(4), 904–908, 1982.

Corey, A. T., *Mechanics of Immiscible Fluids in Porous Media*, 255 pp., Water Resources Publications, Littleton, Colo., 1986.

Dozier, J., Recent research in snow hydrology, *Rev. Geophys.*, *25*(2), 153–161, 1987.

Environmental Protection Agency, Projection of future sea level rise, *Rep. EPA 230-09-007*, 121 pp., Washington, D. C., 1983.

Gerdel, R. W., The transmission of water through snow, *Eos Trans. AGU*, *35*, 475–485, 1954.

Gornitz, V., S. Lebedeff, and J. Hansen, Global sea level trend in the past century, *Science*, *215*, 1611–1614, 1982.

Jordan, P., Meltwater movement in a deep snowpack, 1, Field observations, *Water Resour. Res.*, *19*(4), 971–978, 1983*a*.

Jordan, P., Meltwater movement in a deep snowpack, 2, Simulation model, *Water Resour. Res.*, *19*(4), 979–985, 1983*b*.

Male, D. H., and D. M. Gray, Snowcover ablation and runoff, in *Handbook of Snow*, edited by D. M. Gray and D. H. Male, 776 pp., Pergamon, New York, 1981.

Marsh, P., Ripening processes and meltwater movement in Arctic snowpacks, Ph.D. thesis, 179 pp., McMaster Univ., Hamilton, Ontario, 1982.

Marsh, P., and M.-K. Woo, Wetting front advance and freezing of meltwater within a snow cover, 1, Observations in the Canadian Arctic, *Water Resour. Res.*, *20*(12), 1853–1864, 1984*a*.

Marsh, P., and M.-K. Woo, Wetting front advance and freezing of meltwater within a snow cover, 2, A simulation model, *Water Resour. Res.*, *20*(12), 1865–1874, 1984*b*.

Marsh, P., and M.-K. Wood, Meltwater movement in natural heterogeneous snow covers, *Water Resour. Res.*, *21*(11), 1710–1716, 1985.

Meier, M. F., Contribution of small glaciers to global sea level, *Science*, *226*(4681), 1418–1421, 1984.

National Research Council, *Glaciers, Ice Sheets, and Sea Level: Effect of a CO_2-induced Climate Change*, 330 pp., National Academy Press, Washington, D. C., 1985.

Ozisik, M. N., *Heat Conduction*, 687 pp., John Wiley, New York, 1980.

Shimizu, H., Air permeability of deposited snow, *Contrib. Inst. Low Temp. Sci.*, *A22*, 1–32, 1970.

U. S. Nuclear Regulatory Commission, Documentation and user's guide: UNSAT2—Variable saturated flow model, *Rep. NUREG/CR-3390*, 1983.

Walter, R. J., Jr., and T. H. Illangasekare, User's manual for computer program INSNOW: Infiltration into snow, version 1.0, *Rep. WREEII. 8801*, Dep. of Civ., Environ. and Architect. Eng., Univ. of Colo., Boulder, 1988.

Wankiewicz, A., A review of water movement in snow, in *Modeling of Snow Cover Runoff, Proceedings of Conference on Modeling of Snow Cover Runoff*, edited by S. C. Colbeck and M. Ray, pp. 222–252, U.S. Army Cold Regions Research and Engineering Laboratory, Hanover, N. H., 1979.

T. H. Illangasekare and R. J. Walter, Jr., Department of Civil, Environmental and Architectural Engineering, Engineering Center OT 4-21, Campus Box 428, University of Colorado, Boulder, CO 80309.

M. F. Meier and W. T. Pfeffer, Institute for Arctic and Alpine Research, Campus Box 450, University of Colorado, Boulder, CO 80309.

(Received April 26, 1989;
revised October 6, 1989;
accepted October 12, 1989.)